JOINT EUROPEAN TORUS JET

JET–P(89)32

D.F.H. Start, V.P. Bhatnagar, G. Bosia, D.A. Boyd, M. Bures, D.J. Campbell, J.P. Christiansen, J.G. Cordey, G.A. Cottrell, G. Devillers, L.G. Eriksson, M. P. Evrard, J.A. Heikkinen, T. Hellsten, J. Jacquinot, O.N. Jarvis, S. Knowlton, P. Kupschus, H. Lean, P.J. Lomas, C. Lowry, P. Nielsen, J. O'Rourke, G. Sadler, G.L. Schmidt, A. Tanga, A. Taroni, P.R. Thomas, K. Thomsen, B. Tubbing, M. von Hellermann, U. Willén and JET Team

Physics of High Power ICRH on JET

Physics of High Power ICRH on JET

D.F.H. Start[1], V.P. Bhatnagar[1], G. Bosia[1], D.A. Boyd[2], M. Bures[1], D.J. Campbell[1], J.P. Christiansen[1], J.G. Cordey[1], G.A. Cottrell[1], G. Devillers[1], L.G. Eriksson[3], M. P. Evrard[4], J.A. Heikkinen[1],T. Hellsten[1], J. Jacquinot[1], O.N. Jarvis[1], S. Knowlton[1], P. Kupschus[1], H. Lean[5], P.J. Lomas[1], C. Lowry[1], P. Nielsen[1], J. O'Rourke[1], G. Sadler[1], G.L. Schmidt[6], A. Tanga[1], A. Taroni[1], P.R. Thomas[1], K. Thomsen[1], B. Tubbing[1], M. von Hellermann[1], U. Willén[3] and JET Team*

JET-Joint Undertaking, Culham Science Centre, OX14 3DB, Abingdon, UK

[1]JET Joint Undertaking, Abingdon, Oxon, OX14 3EA, UK
[2]University of Maryland, College Park, Maryland USA
[3]Chalmers University, Gothenburg, Sweden
[4]LPP–ERM/KMS, EUR–EB Association 1040 Brussells Belgium
[5]Culham Laboratory, Abingon, Oxon, OX14 3DB, UK
[6]Princeton Plasma Physics Laboratory, New Jersey USA
** See Appendix 1*

Preprint of Paper to be presented at 8th Topical Conference on
Radio Frequency Power in Plasmas, Irvine, U.S.A. 1st–3rd May 1989

PHYSICS OF HIGH POWER ICRH ON JET

D.F.H. Start, V.P. Bhatnagar, G. Bosia, D.A. Boyd[1], M. Bures, D.J. Campbell, J.P. Christiansen, J.G. Cordey, G.A. Cottrell, G. Devillers, L.G. Eriksson[2], M.P. Evrard[3], J.A. Heikkinen, T. Hellsten, J. Jacquinot, O.N. Jarvis, S. Knowlton, P. Kupschus, H. Lean[4], P.J. Lomas, C. Lowry, P. Nielsen, J. O'Rourke, G. Sadler, G.L. Schmidt[5], A. Tanga, A. Taroni, P.R. Thomas, K. Thomsen, B. Tubbing, M. von Hellermann, U. Willén[2]

JET Joint Undertaking, Abingdon, Oxon, OX14 3EA, UK
[1] University of Maryland, College Park, Maryland USA
[2] Chalmers University, Gothenburg, Sweden
[3] LPP-ERM/KMS, EUR-EB Association 1040 Brussells Belgium
[4] Culham Laboratory, Abingdon, Oxon, OX14 3DB, UK
[5] Princeton Plasma Physics Laboratory, New Jersey USA

ABSTRACT

Ion Cyclotron Resonance Heating (ICRH) experiments have been carried out in a wide range of JET plasmas. A high confinement region in the plasma core has been discovered during on-axis heating of pellet fuelled discharges. Sawtooth-free periods and improved heating efficiency have been achieved in high current plasmas by heating during the current rise. Combined ICRH and neutral beam injection (NBI) in double null X-point plasmas has yielded D-D fusion rates up to $2\times10^{16}s^{-1}$ and electron and ion temperatures of 11keV and 17keV respectively. Non-thermal fusion reaction rates from (He^3)D minority ICRH have been reproduced by a model which predicts $Q \sim 0.7$ for (D)T minority ICRH in JET. RF modulation studies have yielded power deposition profiles and heat transport coefficients inside the q=1 surface. Alignment of the antenna screen to the magnetic field minimises nickel impurity release.

INTRODUCTION

ICRH on JET is provided by 8 antennae situated on the median plane on the low field side of the machine. Each antenna consists of two vertical strip lines with centres separated by 0.31m toroidally and carrying currents with either zero (monopole) or π (dipole) phase difference. Also, the phases between antennae can be imposed to provide a phased array for future fast wave current drive experiments. This array has already proved useful as a 'super dipole' with zero phasing between strip lines in each antennae but π phasing between adjacent antennae. The resulting $k_{||}$ spectrum produces a coupling resistance and nickel impurity release intermediate between those with the normal dipole and monopole phasings.

The system operates in the 23MHz to 57MHz frequency range with a generator power capability of 30MW. So far a maximum of 18MW has been coupled to the plasma, the principle limitation being breakdown in the vacuum lines which have been redesigned for the next operat-

ing period. An automatic matching system which controls the frequency can track rapid changes in antenna/plasma coupling due to density variations or radial eigenmode excitation. This fast system is being augmented by a slow system which controls the tuning stubs and which will almost completely automate the matching process. The Faraday screens of the antennae are water cooled which has allowed long pulse operation to be demonstrated with 6MW of power being coupled for 20 sec with no deleterious effects. However, eventually four antenna have developed leaks as a result of mechanical failure of supporting blocks due to disruptions. These blocks are now strengthened. New beryllium screens (September 1989) will allow long pulse operation to resume.

This paper is a summary of the principal results obtained with ICRF during 1988. In the next section we discuss edge effects, specifically nickel impurity release and parametric decay of the fast wave. In section 3 we present measurements of the power deposition profile, the direct electron heating fraction and the electron thermal diffusivity inside the $q = 1$ surface from RF modulation studies during Monster sawteeth. In section 4 we report on the achievements of on-axis ICRH in high performance scenarios, involving pellet fuelling, RF heating in the current rise and in double null X-point discharges. Finally in section 5 we use a model, validated by (He^3,D) fusion yield experiments, to predict non-thermal (D,T) Q values for JET with (D)T ICRH minority heating.

EDGE EFFECTS: NICKEL IMPURITIES AND PARAMETRIC DECAY WAVES

Previous experiments have shown that nickel is released only from the screens of energised antennae suggesting that local RF fields play a role[1]. However the perpendicular electric field of the fast wave is probably not responsible since the influx does not correlate with eigenmode excitation[2]. On the other hand, non-alignment of the screen elements with the magnetic field B allows a parallel component, $E_{||}$, to penetrate into the edge plasma and possibly accelerate ions into the screen to release nickel by sputtering. The screen elements on JET are aligned to within $\sim 5°$ under normal operating conditions. On-axis (H)D heating experiments at $I_p = 2MA$, $B_T = 2.1T$ used both normal and reversed toroidal field directions which gave screen angles of 5° and 25° to B. The intensity of the NiXXVI line was three-fold enhanced by this increase in angle. Moreover, the coupling resistance, electron temperature and incremental confinement time were all reduced by 30% in the reversed field case. Such reduced performance implies a smaller power fraction coupled to the fast wave with perhaps increased excitation of the slow wave as the screening of $E_{||}$ becomes less effective. Either this or near field effects (sheath rectification) could cause nickel influx.

Probe measurements in the plasma edge have detected parametric decay of the fast wave into two slow waves or into a Bernstein wave and a quasi-mode. An example is shown in Fig. 1. Spectra were recorded at several RF power levels in a 3MA, 3.15T discharge

containing a mixed D, He^3 plasma with H-minority ions. The RF frequency was 48MHz to give on-axis heating, the phasing was monopole and the toroidal field direction was normal. As the RF power is increased, peaks emerge which can be identified as quasi-modes for deuterium and He^3 with their corresponding Ion Bernstein Waves (IBW). In this example any decay to the slow waves at 24MHz is obscured but has been seen when the IBW branch is forbidden.

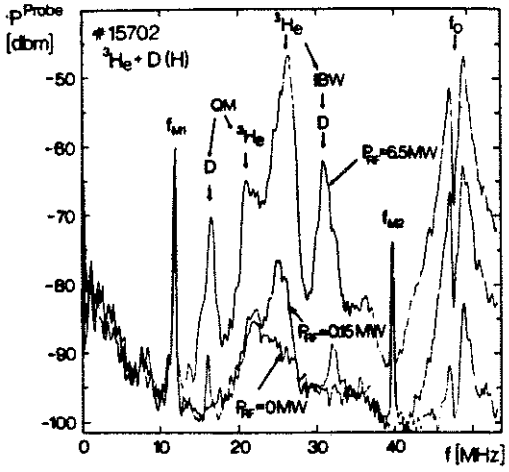

Fig. 1. Parametric Decay Waves in JET Edge Plasma

RF MODULATION DURING MONSTER SAWTEETH

The response of the central electron temperature, $T_e(0)$ to 4Hz square wave modulation of central He^3 minority ICRH between 6MW and 8.5MW is shown in Fig. 2. The discharge parameters were I_p = 2MA, B_T = 3.4T, $n_e(0) = 4.2 \times 10^{19} m^{-3}$ and the He^3 concentration was 5% of the electron density. The sharp change in the derivative of $T_e(0)$ at the RF switch up (switch down) is due to the modulated direct electron heating. Direct heating occurs through mode conversion, electron Landau damping or TTMP; indirect electron heating arises from friction with the minority ions. The magnitude of the discontinuity in $\partial T_e(0)/\partial t$ gives a modulated direct heating power density of $50 kW/m^3$ in the plasma centre. The amplitude profile of the 4Hz component of T_e is almost gaussian with a peak value of 200eV on- axis and with a width of 0.3m. The phase delay between the T_e oscillation and the power modulation is 82 ± 5° in the centre and increases monotonically towards the limiter. The phase and amplitude profiles were analysed using a simple electron heat diffusion model to obtain a thermal diffusivity $1.5 < \chi_e(m^2 s^{-1}) < 3.0$, a gaussian power deposition width of 0.18 ± 0.04m and a direct heating fraction of 10 ± 3%. This localised heating agrees well with self consistent full wave/Fokker-Planck calculations.

With lower He^3 concentration (2%) and higher average power, (10MW compared with 7.2MW), the T_e response is quite different to that above. The amplitude profile is hollow at 4 Hz modulation but peaked at 16Hz (Fig. 3). A hollow profile suggests off-axis heating (although the minority resonance layer was central) except that the phase delay is least on-axis. These data can be reproduced, however, if there is a depletion of the minority heating on-axis as the power is increased, such as could occur if the width of the minority heating profile were modulated. The required fractional change in the profile width is about 4% which is similar to the calculated oscillating minority energy fraction and could perhaps arise from a modulation of the banana orbits. This interpretation is clearly not unique and another possibility has appeared recently

from studies of the minority Fokker Planck equation with a modulated power source. The phase of the power transferred to the electrons is found to be delayed by $\sim \pi/2$ at low and high energies but is advanced by $\sim \pi/2$ at energies around the tail temperature. The data could then be readily explained if this latter component dominates the heating on-axis due to orbit effects.

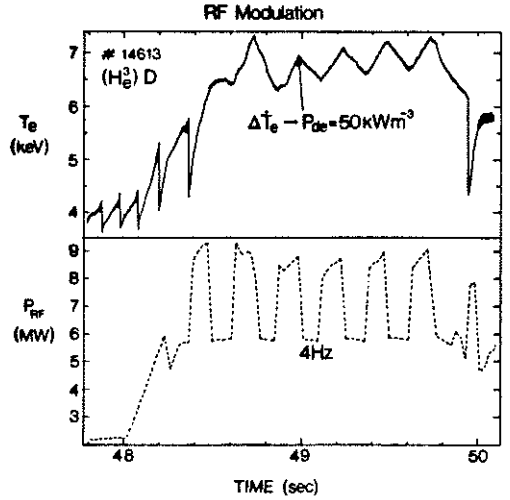

Fig. 2. T_e Response to RF Power Modulation

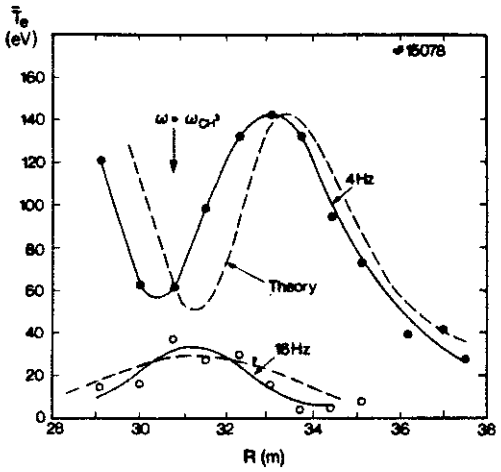

Fig. 3. Radial Profile of Modulated T_e

HIGH PERFORMANCE SCENARIOS

PELLET FUELLED DISCHARGES Plasmas with peaked density profiles produced by pellets have been successfully heated with H-minority ICRF without the density pump-out observed in previous experiments. The time evolution of plasma parameters in a 3MA, 3.3T discharge is shown in Fig. 4. Pellets of 2.7mm diameter were injected at 41.5s and 42s followed by a 4mm pellet at 43s which produced a central density, $n_e(0) = 9\times10^{19}m^{-3}$. The 4mm pellet was closely followed by 5MW of neutral beam power and $\sim$ 13MW of ICRF hydrogen minority heating, which raised $T_e(0)$ to 12keV at 44.25s when a sudden collapse

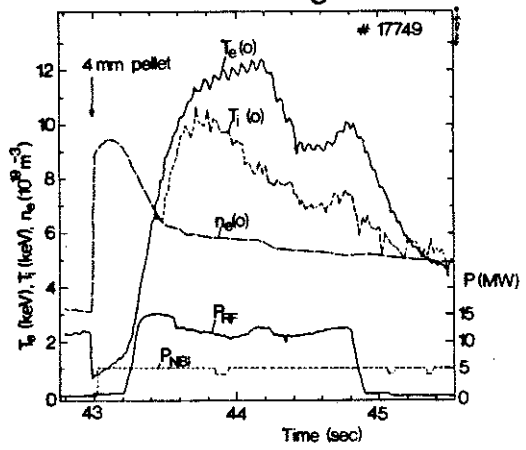

Fig. 4. Time Evolution of Pellet Fuelled Plasma

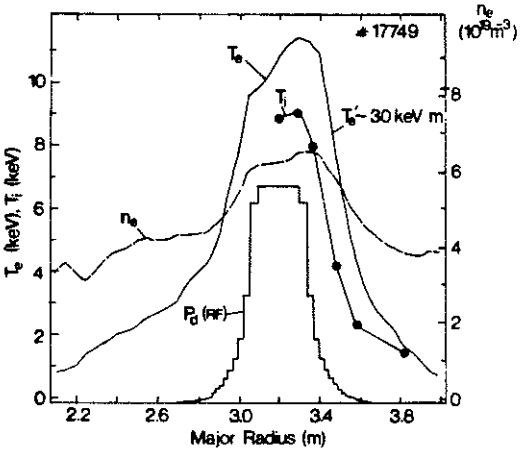

Fig. 5. Radial Profiles at t = 44.2 sec

occurred. The central ion temperature, $T_i(0)$, from doppler broadening of NiXXVII radiation, initially increased to 10keV at 43.8s and slowly decayed thereafter. The NBI allowed $T_i(r)$ profiles to be measured by charge exchange spectroscopy[3] as shown in Fig. 5 for t = 44.2 sec. Also shown are LIDAR profiles of T_e and n_e, the latter remaining peaked although the central density is much less than that just after pellet injection. The $T_e(r)$ and $T_i(r)$ profiles are extremely peaked even by comparison with those during monster sawteeth and the strong gradients imply enhanced confinement. For diffusive heat loss the electron power balance at minor radius a in cylindrical geometry can be written

$$P_e = 4\pi^2 R a n_e(a) \chi_e(a) \left.\frac{\partial T_e}{\partial r}\right|_a$$

where P_e is the power input to electrons within the radius a, R is the major radius and χ_e the thermal diffusivity. According to ray tracing, most of the power is deposited inside a = 0.35m (see Fig. 5). From the T_e gradient and the calculated ICRF power flow to the electrons (69%) we estimate $\chi_e \sim 0.8 m^2/s$. This value is a factor 2-3 less than those obtained for monster sawteeth. This estimate is confirmed by detailed transport calculations[4] which find that the improvement extends over the inner half radius where $\chi_e \sim 0.8 m^2/s$ and $\chi_i \sim 0.6 m^2/s$. Outside this region the values of χ_e and χ_i are higher by factors of 2 and 4 respectively.

Statistical comparisons of this improved confinement regime with non-peaked density profile discharges (including plasmas with monster sawteeth) show that $T_i(0)$ and $T_e(0)$ are factors of 2 and 1.4 higher, respectively, for the same value of $P_{total}/n_e(0)$. Also the D-D fusion reaction rate is a factor of 4 larger, but the global energy confinement is only increased by 20%. The fusion parameter $n_D(0)T_i(0)\tau_E$ reaches $2 \times 10^{20} keV m^{-3} s$ which is comparable with values in good H-mode plasmas. The strong pressure gradients produced bootstrap currents of the order of 0.8 MA[5] which, together with the initial cooling by the pellet, tend to broaden the current profile: equilibrium analysis gives a value of q(0) close to 1.5 prior to the crash. After the crash there is a strong increase in n = 2 MHD activity with an odd poloidal mode number, $m \geq 3$. Theoretical studies suggest that ballooning modes[6] or modes with intermediate n values[7] ('infernal' modes) could cause the collapse.

CURRENT RISE HEATING ICRH hydrogen minority heating of deuterium plasmas has been applied on-axis during the current rise of 5 MA and 6 MA discharges in order to heat the plasma before or shortly after the onset of sawteeth. For I_p = 5MA the retarded current penetration delayed the first sawtooth collapse by up to 1.2 s. This collapse occurred for $q(0) \sim 1$ according to polarimetry data. With 11 MW of RF power the central electron temperature reached 10.5 keV for $n_e(0) = 6 \times 10^{19} m^{-3}$ just prior to the collapse. The temperature profile was highly peaked, $T_e(0)/\langle T_e \rangle \sim 3$-4 and the discharges were particularly clean with $Z_{eff} \sim 2$. The 6 MA discharges exhibited small sawteeth before the heating pulse which, for $P_{RF} > 6$ MW, produced a monster sawtooth as the current reached 5 MA. Current

rise heating is the only way monster sawteeth have been produced in such high current discharges. Fig. 6 shows the larger values of $n_e(0) \cdot T_e(0)$ during the current rise compared with those obtained

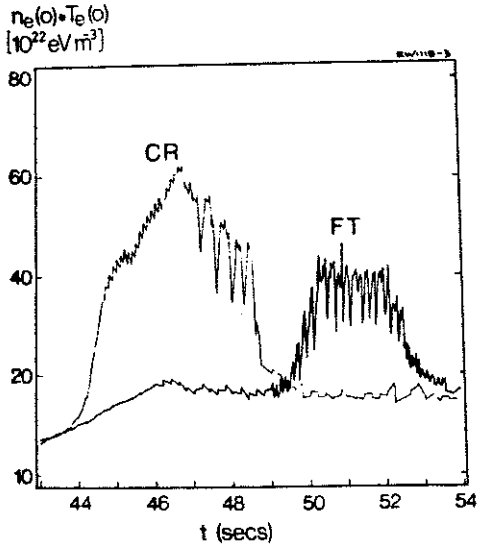

Fig. 6. Current Rise and Flat Top Heating for I_p = 5MA

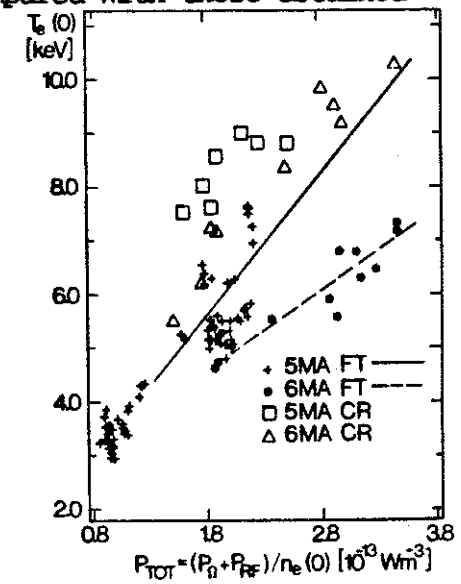

Fig. 7. $T_e(0)$ During Current Rise and Flat Top Heating

during the flat top. This improvement stems from the enhanced $T_e(0)$. A statistical comparison of current rise and flat top values of $T_e(0)$ plotted against $P_{total}/n_e(0)$ is shown in Fig. 7 for both I_p = 5 MA and I_p = 6 MA. Similar comparisons for other parameters lead to the following summary of the enhancements obtained with current rise heating.

1) A 50% increase in $T_e(0)$ for equal values of $P_{total}/n_e(0)$.
2) 10-20% improvement in $T_i(0)$ in both 5 MA and 6 MA plasmas.
3) An increase in the global energy confinement by typically 15% due to the suppression of the sawteeth.
4) Twofold enhancement of the D-D fusion rate in 5 MA plasmas partly due to second harmonic heating of deuterium.

The best values of the fusion parameter achieved so far is $n_D(0)T_i(0)\tau_E=1.65\times10^{20}(m^{-3}keVsec)$. This scenario appears to be the most suitable for ICRH (D)T operation as discussed in section 5.

DOUBLE NULL X-POINT DISCHARGES Combined NBI ($\leq$ 21MW) and ICRH ($\leq$ 11MW) experiments have obtained D-D reaction rates up to $2\times10^{16}s^{-1}$ in 3MA, 3.2T double null X-point deuterium plasmas. This configuration was chosen for good density control through the pumping action of the X-point carbon tiles and for good matching of the plasma boundary to the RF antenna curvature[8]. The deuterium beam energy was $\sim$ 80keV and the 48MHz, on-axis ICRH used hydrogen minority ions. The pre-heating target density was $\sim 1.5\times10^{19}m^{-3}$ but increased during the heating pulse, thereby contributing to a non-steady neutron production, principally from beam-plasma inter actions, which reached a maximum for $n_e(0) \sim 3\times10^{19}m^{-3}$. Values of $T_e(0)$ and $T_i(0)$ up to 11keV and 17keV respectively were achieved. A

plot of reaction rate versus NBI power, in Fig. 8, shows the enhancement with combined heating compared with beam-only cases. TRANSP code simulations show that this enhancement is not solely due to the improved plasma parameters, notably T_e, when RF is applied. This conclusion implies an acceleration of the beam ions by second harmonic heating although neutron spectroscopy reveals the presence of only a weak tail above 80keV.

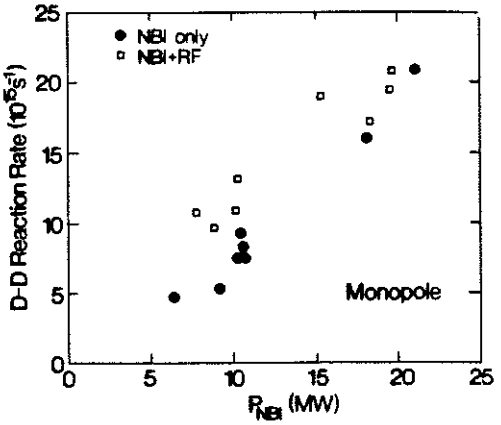

Fig. 8. D-D Fusion Rate for NBI + RF and NBI Only

During these experiments, several H-modes were formed and in one case (# 18773) the limiter clearance was only 1cm compared with 3cm normally required for H-modes. This discharge was fuelled with three 2.7mm pellets and then heated with 10MW of ICRF and 15MW of NBI during which a 3MA to 3.5MA current ramp was applied. The confinement time was $\sim$ 0.6s (twice the Goldston L-mode value), the energy content was 11MJ, $T_e(0)$ and $T_i(0)$ were close to 10keV and the D-D reaction rate reached $1.9 \times 10^{16} s^{-1}$. The proximity of the plasma gave good coupling ($R_c \sim 6\Omega$) and the radiated power rise rate was low ($\sim 5 MWs^{-1}$) compared with previous NBI + RF heated H-modes ($\sim 10 MWs^{-1}$) indicating a low influx of nickel. In Fig. 9 the energy content, W, is compared with values for NBI alone and NBI + RF in 3MA H-modes. The upper and lower curves are 2 x Goldston scaling for I_p = 3.5MA and 3MA, respectively. This type of discharge will be investigated further during the next experimental campaign.

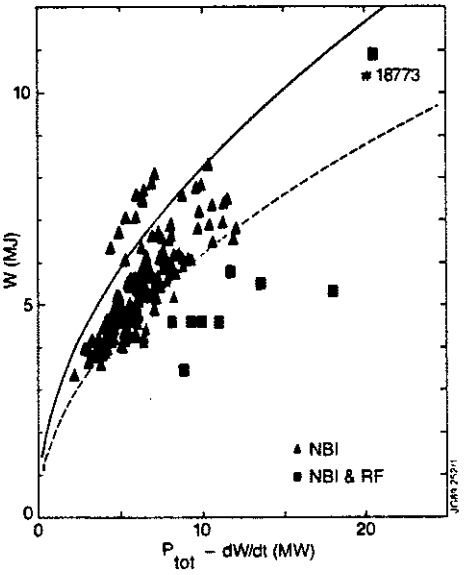

Fig. 9. Energy Content in 3MA H-modes

NON THERMAL FUSION FROM (D)T MINORITY ICRH

Experiments using He^3 minority ICRH in deuterium plasmas have yielded up to 60kW of fusion power from He^3-D fusion reactions[8]. The results, particularly the scaling with RF power, have been simulated using both a Stix model[9] and a self consistent full wave/-Fokker Planck treatment[10]. In this section we describe predictions of the Stix model for the D-T fusion yield from fundamental ICRF heating of deuterium in tritium JET plasmas. The plasma parameters are based on those attained in high performance scenarios with;

a) pellet injection at 3MA, b) current rise heating at 5MA and c) monster sawteeth at 3MA. In the model, the profiles of $n_e(r)$ and $T_e(r)$ were parabolic to a power γ which was determined by fitting experimental data. Central values, $n_e(0)$ and $T_e(0)$, were extrapolated to high power levels ($\sim$ 20MW) using the measured offset linear scaling laws of the type $T_e(0) = \alpha + \beta P_{tot}/n_e(0)$ as shown in Fig. 7. We also assume $T_i = T_e$ which is not fully justified experimentally. However, T_i approaches T_e in the pellet fuelled discharges which have central densities close to that for which the (D)T scheme is optimum. The RF power absorption was investigated by ray tracing for f = 25MHz, B_T = 3.55T and dipole antennae phasing. For example, with 30% deuterium minority, the pellet fuelled discharge parameters gave 80% single pass absorption on deuterium, 17% direct electron heating (TTMP + ELD) and 3% was unabsorbed. In the Stix model the power deposition was taken as gaussian with a width of 0.2m. The predicted fusion yields are plotted against $n_e(0)$ in Fig. 10 for 20MW of power coupled to the minority ($P_{RF} \sim$ 24MW), n_D/n_e = 15% and 30%, Z_{eff} = 2, and off-axis heating ($r \sim 0.3$m). The fusion yield peaks for densities close to $1\times10^{20}m^{-3}$ when the minority tail temperature is optimum ($T_{tail} \sim$ 140keV). For this case of fixed Z_{eff} the pellet fuelled discharges and the current rise heating give similar values of Q_{RF}(= P_{Fusion}/P_{RF}) = 70%. However, only the current rise heating achieved Z_{eff} = 2. With pellets Z_{eff} was about 3 for maximum $T_e(0)$ and this further dilution reduces Q_{RF} to 50%.

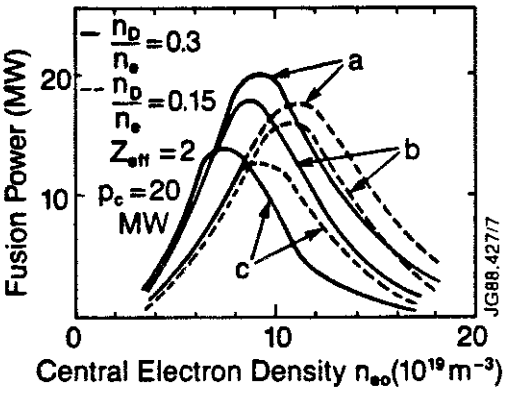

Fig. 10. Predicted Fusion Power for (D)T Minority ICRH

SUMMARY

ICRH has made a major contribution to high performance JET plasmas. Its strongly localised nature, as verified by modulation studies, allowed heating well within the central enhanced confinement region in peaked denisty plasmas and has generated sawtooth-free periods during the current rise phase of 5MA and 6MA discharges. Previously encountered problems of ICRF heating of H-modes (low coupling, impurity influxes) appear to be absent in a new scenario allowing 1cm plasma/limiter separation in double-null X-point discharges. Further investigation of this scenario, together with a) (H)D and (He^3)D experimental simulations of the (D)T high Q scheme, b) fast wave and minority ion current drive studies and c) investigation of synergism with combined RF and NBI, will all be essential elements in the near term development of ICRH on JET.

ACKNOWLEDGEMENTS

It is a pleasure to acknowledge the assistance of all our colleagues in the JET team. Particular thanks go to the tokamak operating team, the RF and NBI operating teams and to the members of the diagnostic groups contributing to these measurements.

REFERENCES

1. M. Bures et al, Plasma Physics and Cont. Fusion 30(1988) 149.
2. J. Jacquinot et al, Plasma Physics and Cont. Fusion 30(1988)1467.
3. M. von. Hellermann et al, 16th Eur. Conf. on Contr. Fusion and Plasma Physics, Venice 1989.
4. V.P. Bhatnagar et al, ibid.
5. P. Stubberfield et al, ibid.
6. R.M.O. Galvão et al, ibid.
7. L.A. Charlton et al, Proc. of 1989 Int. Sherwood Theory Conf., Texas 1989, paper 2C27.
8. B. Tubbing et al, 16th Eur. Conf. on Fusion and Plasma Physics, Venice 1989.
9. D.A. Boyd et al, to be published in Nuclear Fusion.
10. L.G. Eriksson et al, Nuclear Fusion 29(1989)87.

APPENDIX 1.

THE JET TEAM

JET Joint Undertaking, Abingdon, Oxon, OX14 3EA, U.K.

J.M.Adams[1], F.Alladio[4], H.Altmann, R.J.Anderson, G.Appruzzese, W.Bailey, B.Balet, D.V.Bartlett, L.R.Baylor[24], K.Behringer, A.C.Bell, P.Bertoldi, E.Bertolini, V.Bhatnagar, R.J.Bickerton, A.Boileau[3], T.Bonicelli, S.J.Booth, G.Bosia, M.Botman, D.Boyd[31], H.Brelen, H.Brinkschulte, M.Brusati, T.Budd, M.Bures, T.Businaro[4], H.Buttgereit, D.Cacaut, C.Caldwell-Nichols, D.J.Campbell, P.Card, J.Carwardine, G.Celentano, P.Chabert[27], C.D.Challis, A.Cheetham, J.Christiansen, C.Christodoulopoulos, P.Chuilon, R.Claesen, S.Clement[30], J.P.Coad, P.Colestock[6], S.Conroy[13], M.Cooke, S.Cooper, J.G.Cordey, W.Core, S.Corti, A.E.Costley, G.Cottrell, M.Cox[7], P.Cripwell[13], F.Crisanti[4], D.Cross, H.de Blank[16], J.de Haas[16], L.de Kock, E.Deksnis, G.B.Denne, G.Deschamps, G.Devillars, K.J.Dietz, J.Dobbing, S.E.Dorling, P.G.Doyle, D.F.Düchs, H.Duquenoy, A.Edwards, J.Ehrenberg[14], T.Elevant[12], W.Engelhardt, S.K.Erents[7], L.G.Eriksonn[5], M.Evrard[2], H.Falter, D.Flory, M.Forrest[7], C.Froger, K.Fullard, M.Gadeberg[11], A.Galetsas, R.Galvao[8], A.Gibson, R.D.Gill, A.Gondhalekar, C.Gordon, G.Gorini, C.Gormezano, N.A.Gottardi, C.Gowers, B.J.Green, F.S.Griph, M.Gryzinski[26], R.Haange, G.Hammett[6], W.Han[9], C.J.Hancock, P.J.Harbour, N.C.Hawkes[7], P.Haynes[7], T.Hellsten, J.L.Hemmerich, R.Hemsworth, R.F.Herzog, K.Hirsch[14], J.Hoekzema, W.A.Houlberg[24], J.How, M.Huart, A.Hubbard, T.P.Hughes[32], M.Hugon, M.Huguet, J.Jacquinot, O.N.Jarvis, T.C.Jernigan[24], E.Joffrin, E.M.Jones, L.P.D.F.Jones, T.T.C.Jones, J.Källne, A.Kaye, B.E.Keen, M.Keilhacker, G.J.Kelly, A.Khare[15], S.Knowlton, A.Konstantellos, M.Kovanen[21], P.Kupschus, P.Lallia, J.R.Last, L.Lauro-Taroni, M.Laux[33], K.Lawson[7], E.Lazzaro, M.Lennholm, X.Litaudon, P.Lomas, M.Lorentz-Gottardi[2], C.Lowry, G.Magyar, D.Maisonnier, M.Malacarne, V.Marchese, P.Massmann, L.McCarthy[28], G.McCracken[7], P.Mendonca, P.Meriguet, P.Micozzi[4], S.F.Mills, P.Millward, S.L.Milora[24], A.Moissonnier, P.L.Mondino, D.Moreau[17], P.Morgan, H.Morsi[14], G.Murphy, M.F.Nave, M.Newman, L.Nickesson, P.Nielsen, P.Noll, W.Obert, D.O'Brien, J.O'Rourke, M.G.Pacco-Düchs, M.Pain, S.Papastergiou, D.Pasini[20], M.Paume[27], N.Peacock[7], D.Pearson[13], F.Pegoraro, M.Pick, S.Pitcher[7], J.Plancoulaine, J-P.Poffé, F.Porcelli, R.Prentice, T.Raimondi, J.Ramette[17], J.M.Rax[27], C.Raymond, P-H.Rebut, J.Removille, F.Rimini, D.Robinson[7], A.Rolfe, R.T.Ross, L.Rossi, G.Rupprecht[14], R.Rushton, P.Rutter, H.C.Sack, G.Sadler, N.Salmon[13], H.Salzmann[14], A.Santagiustina, D.Schissel[25], P.H.Schild, M.Schmid, G.Schmidt[6], R.L.Shaw, A.Sibley, R.Simonini, J.Sips[16], P.Smeulders, J.Snipes, S.Sommers, L.Sonnerup, K.Sonnenberg, M.Stamp, P.Stangeby[19], D.Start, C.A.Steed, D.Stork, P.E.Stott, T.E.Stringer, D.Stubberfield, T.Sugie[18], D.Summers, H.Summers[20], J.Taboda-Duarte[22], J.Tagle[30], H.Tamnen, A.Tanga, A.Taroni, C.Tebaldi[23], A.Tesini, P.R.Thomas, E.Thompson, K.Thomsen[11], P.Trevalion, M.Tschudin, B.Tubbing, K.Uchino[29], E.Usselmann, H.van der Beken, M.von Hellermann, T.Wade, C.Walker, B.A.Wallander, M.Walravens, K.Walter, D.Ward, M.L.Watkins, J.Wesson, D.H.Wheeler, J.Wilks, U.Willen[12], D.Wilson, T.Winkel, C.Woodward, M.Wykes, I.D.Young, L.Zannelli, M.Zarnstorff[6], D.Zasche[14], J.W.Zwart.

PERMANENT ADDRESS

1. UKAEA, Harwell, Oxon. UK.
2. EUR-EB Association, LPP-ERM/KMS, B-1040 Brussels, Belgium.
3. Institute National des Récherches Scientifique, Quebec, Canada.
4. ENEA-CENTRO Di Frascati, I-00044 Frascati, Roma, Italy.
5. Chalmers University of Technology, Göteborg, Sweden.
6. Princeton Plasma Physics Laboratory, New Jersey, USA.
7. UKAEA Culham Laboratory, Abingdon, Oxon. UK.
8. Plasma Physics Laboratory, Space Research Institute, Sao José dos Campos, Brazil.
9. Institute of Mathematics, University of Oxford, UK.
10. CRPP/EPFL, 21 Avenue des Bains, CH-1007 Lausanne, Switzerland.
11. Risø National Laboratory, DK-4000 Roskilde, Denmark.
12. Swedish Energy Research Commission, S-10072 Stockholm, Sweden.
13. Imperial College of Science and Technology, University of London, UK.
14. Max Planck Institut für Plasmaphysik, D-8046 Garching bei München, FRG.
15. Institute for Plasma Research, Gandhinagar Bhat Gujat, India.
16. FOM Instituut voor Plasmafysica, 3430 Be Nieuwegein, The Netherlands.
17. Commissiariat à L'Energie Atomique, F-92260 Fontenay-aux-Roses, France.
18. JAERI, Tokai Research Establishment, Tokai-Mura, Naka-Gun, Japan.
19. Institute for Aerospace Studies, University of Toronto, Downsview, Ontario, Canada.
20. University of Strathclyde, Glasgow, G4 ONG, U.K.
21. Nuclear Engineering Laboratory, Lapeenranta University, Finland.
22. JNICT, Lisboa, Portugal.
23. Department of Mathematics, Univeristy of Bologna, Italy.
24. Oak Ridge National Laboratory, Oak Ridge, Tenn., USA.
25. G.A. Technologies, San Diego, California, USA.
26. Institute for Nuclear Studies, Swierk, Poland.
27. Commissiariat à l'Energie Atomique, Cadarache, France.
28. School of Physical Sciences, Flinders University of South Australia, South Australia SO42.
29. Kyushi University, Kasagu Fukuoka, Japan.
30. Centro de Investigaciones Energeticas Medioambientales y Techalogicas, Spain.
31. University of Maryland, College Park, Maryland, USA.
32. University of Essex, Colchester, UK.
33. Akademie de Wissenschaften, Berlin, DDR.

CR 88.49.1A